SAND74-0124
Unlimited Release

Design Analysis of Asymmetric Solar Receivers

W. H. McCulloch, G. W. Treadwell

Prepared by Sandia Laboratories, Albuquerque, New Mexico 87115
and Livermore, California 94550 for the United States Atomic Energy
Commission under Contract AT (29-1)-789

Printed August 1974

Sandia Laboratories
energy report

SF 2900-QQB(3-74)

Issued by Sandia Laboratories, operated for
the United States Atomic Energy Commission by Sandia Corporation

SC 1004-DF (10-70)

SAND74-0124
Unlimited Release
Printed August 1974

DESIGN ANALYSIS OF ASYMMETRIC SOLAR RECEIVERS

W. H. McCulloch
Heat Transfer and Fluid Mechanics Division 1543

G. W. Treadwell
Solar Energy Projects Division 5712

Sandia Laboratories
Albuquerque, New Mexico 87115

ABSTRACT

One of the primary distinctions among parabolic cylinder solar collectors is the focal length of the reflector. For a given collector width, this focal length is directly related to the rim angle. Previous studies have used different criteria to optimize collector designs. This study considers in detail the effects of varying the receiver design with focal length. As the rim angle is decreased, an increasing portion of the receiver and its envelope receives little or no reflected solar flux, and this portion may be designed to minimize thermal losses. The result is a design which is not symmetric about the receiver axis. The purpose of this analysis is to examine the performance of such an asymmetric receiver design and to determine the optimum rim angle.

The results of the study show that, for the receiver configuration and operational conditions described, the optimum receiver has a 90° rim angle. The impact of varying a number of design parameters is also evaluated.

DESIGN ANALYSIS OF ASYMMETRIC SOLAR RECEIVERS

I. Introduction

The effective utilization of thermal energy derived from incident sunlight often requires that the solar energy be collected at temperatures which can be achieved only with some degree of concentration. One such concept is the Solar Total Energy Program which has been previously described [1-3].* For that system, the solar energy must be collected at a temperature high enough to operate an organic fluid Rankine turbine for the generation of electricity, and the parabolic cylinder solar collector design has been selected as the most appropriate.

A parabolic cylinder solar collector consists of a parabolic cylinder reflector which focuses the insolation onto a receiver tube where the energy is absorbed in a working fluid. Hassan and El-Refaie [4] present a theoretical study of the performance of a parabolic cylinder reflector as a function of focal length but do not consider the design of a receiver to collect the concentrated energy. The analytical and experimental work of Löf, Fester, and Duffie [5] is an example of other characterizations of the performance of focusing solar collectors with tubular receivers.

Calculations have shown that the performance of tubular receivers can be improved substantially by placing the receiver inside a transparent envelope to reduce both the convection and radiation losses. Pope and Schimmel [6] provide an analysis which includes the consideration of the convective/radiative energy exchange between a receiver and its envelope, the effect of silvering the envelope to reduce radiative losses, and the effect of transmission through the envelope. Their analysis, however, is one-dimensional and as such does not include consideration of the window in the silvered envelope.

One of the primary distinctions among parabolic cylinder solar collectors is the focal length of the reflector. For a fixed aperture, i.e., the distance from one edge of the parabolic reflector to the other, this focal length is directly related to the rim angle as shown in Figure 1. The basic objective of the present study is to determine the rim angle (focal length) for optimum performance. The performance can be characterized by the collector efficiency, defined as the fraction of solar energy intercepted by the collector which is delivered to the working fluid.

---

*Numbers in brackets refer to similarly numbered entries in the list of references.

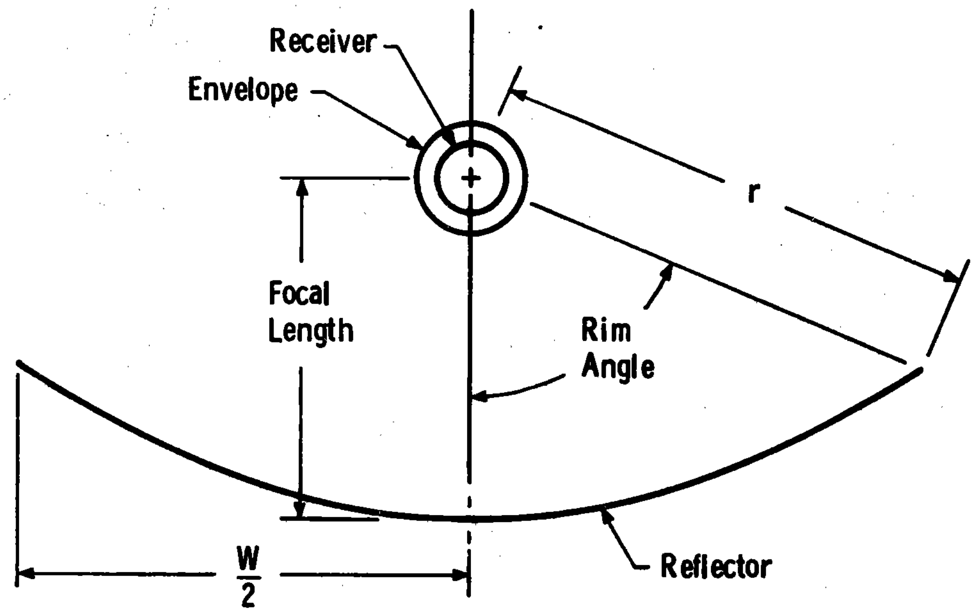

Figure 1. Parabolic cylinder solar collector

Some of the losses are independent of the receiver configuration. The incident radiation is attenuated by the specular reflectivity of the reflector surface, the transmissivity of the envelope, and the absorptivity of the receiver surface. Once the energy is absorbed by the receiver, there are additional thermal losses which can be affected by the receiver design.

Previous efforts to select an optimum rim angle have considered receivers which are symmetrical about their axes. One study [7], which optimizes the rim angle to minimize the effects of reflector aberrations, suggests that rim angles of 115° are best. The computer model developed in another study [8] was used to evaluate receivers whose diameters had been determined by the maximum distance from the reflector surface to the focal line. These calculations indicated that a rim angle of 90° gives better performance due to the smaller receiver diameter.

Symmetrical receivers are designed as if the solar input were to come from all directions onto the entire receiver surface. In some collector configurations an angular segment of the receiver and its envelope is not illuminated appreciably by the reflected solar flux. These surfaces do, however, participate in the mechanisms by which heat is lost from the receiver, and the performance could be improved by reducing these thermal losses by means of such techniques as reflectively coating the inside surface of the envelope and insulating the outside surface. The result is a design which is no longer symmetrical about the axis. The extent to which such thermal protection may be placed on the envelope increases with smaller rim angles.

Preliminary calculations indicated that it is possible to offset the deleterious thermal effect of increasing receiver size with smaller rim angles by going to asymmetric designs which include insulation and silvering on the unilluminated portion of the envelope. The purpose of this analysis is, then, to determine the extent to which insulation and a reflective coating can be included in the receiver design for various rim angles, to examine the comparative performance of such asymmetric receivers for which the collector width is held constant, and to select the optimum rim angle on this basis.

II. Analysis

Thermal Model

To represent the two-dimensional heat transfer problem, a computer program has been developed which constructs a nodal network which models a cross-section of the receiver. The computer program accepts input data which describes the receiver to be analyzed, determines the appropriate data for the numerical representations, and executes a solution utilizing CINDA-3G [9], a general purpose heat transfer code.

The generic description of the nodal model of the receiver is shown in Figure 2. The model represents one half of the receiver which is symmetrical about the line from the vertex of the parabolic cylinder reflector to the focus which is coincident with the center of the receiver. The nodes are defined by dividing the half-section into eight equal segments. Each of the nodes which represents a part of the mass (i.e., a diffusion node) is numbered in Figure 2. In addition there are surface nodes on the inside and outside surfaces of the receiver, the inside surface of the envelope and the outside surface of the insulation.

The inside surface of the receiver transfers heat to the working fluid by convection. The fluid is assumed to be at a uniform temperature. The outside surface of the receiver accepts the solar input, the intensity and distribution of which are discussed below. The receiver exchanges energy with the envelope by radiation and conduction. The radiation heat transfer is treated by a radiosity network solution which requires the emissivity of each surface node and the shape factors which characterize the geometrical configuration. Convection across the annulus between the receiver and envelope can be made negligibly small by selecting a sufficiently small spacing. At the temperatures expected in these solar collectors, an air gap of 0.25 in. satisfies the criterion and is included in each of the designs. Furthermore, most candidate receiver coatings require a controlled atmosphere for long life; and a partial vacuum may be maintained in the gap, also inhibiting convection. However, since a relatively hard vacuum is required to prevent conduction heat transfer, it is assumed that the conduction mode is active. Further consideration of these heat transfer mechanisms is suggested as a possible extension of this study.

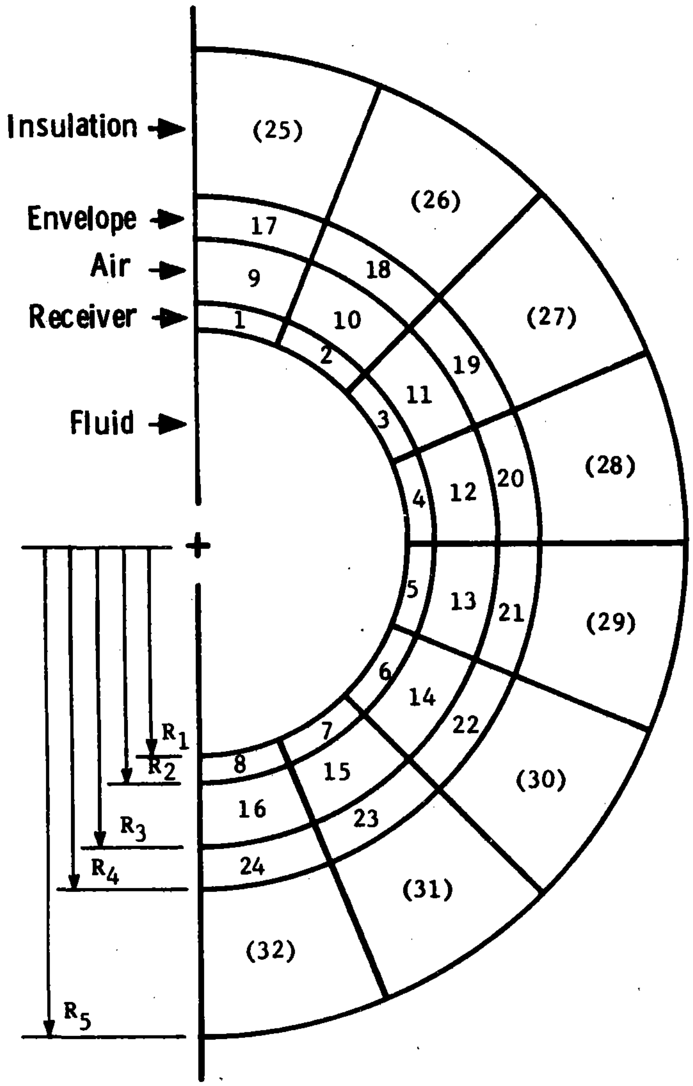

Figure 2. General nodal network

The computer program includes the logic necessary to model the insulation layer over a specified number of segments, counting from the top. Since these nodes may or may not be present physically, their numbers are shown in parentheses in Figure 2. The model assumes that the outermost surface, whether insulation or envelope, loses heat by convection to air and by radiation to the environment.

Input Data

The thermal model described above must be supplied with input data to describe the receiver and its operation. The number of possible combinations of these data approaches infinity. Therefore, it is the purpose of this section to collect a set of meaningful input values to serve as a baseline for the analysis. The impact of parametric variation from this baseline is discussed in a later section.

Although solar energy cannot be regarded as a new idea, good thermophysical property data for engineering materials and surfaces which might be used in mass-produced solar collectors are not plentiful. Also the techniques for measuring these properties and reporting the data have not been standardized. Sandia Laboratories, along with others, is endeavoring to provide reliable data, particularly for the optical properties, for such materials. The properties data for this study have been selected from measurements taken on presently available materials and coatings.

The receiver surface is critical to the performance of the solar collector because it both absorbs the insolation and radiates heat away from the receiver, which is one of the primary loss mechanisms. Therefore, it is important that the receiver surface absorb as completely as possible the short wavelength radiation while concurrently emitting little energy as longer wavelength infrared radiation. Several surfaces which exhibit such behavior are being evaluated, and a sizable portion of current solar energy research is committed to the effort to provide long-lived surfaces with increased absorptivity in the visible and reduced emissivity in the infrared.

Baseline data values for these and other optical properties are given in Table 1. To this point in the study these data have been taken as constants even though the computer program is capable of treating the properties as functions of temperature. Data for the thermal conductivities of the various materials have been selected from those provided by Kreith [10]. For this analysis the receiver is assumed to be steel, the gas inside the envelope to

Table 1. Baseline Input Data

Temperature of the working fluid	600°F
Temperature of the ambient air	77°F
Temperature of the environment	77°F
Receiver surface absorptivity (visible)	0.90
Receiver surface emissivity (infrared)	0.30
Reflector reflectivity	0.78
Envelope transmissivity (visible)	0.90
Envelope emissivity	0.90
Envelope emissivity with silvering	0.20
Insulation surface emissivity	0.20
Convection heat transfer coefficient for air	3.44 Btu/ft^2-hr-F
Convection heat transfer coefficient for working fluid	164 Btu/ft^2-hr-F
Normal solar insolation	318 Btu/ft^2-hr

have the properties of air, the envelope to be window glass, and the insulation to be equivalent to Kreith's entry called "molded pipe covering."

Previous considerations have led to the selection of 600°F as the working temperature of the collector fluid for the Solar Total Energy Project at Sandia Laboratories. With this temperature, preliminary heat balance calculations have established that radiation loss is a weak function of the radiation sink temperature, and 77°F is the baseline ambient temperature for both the radiation loss and the convective loss to the environment.

Since the temperature of the working fluid is 600°F, the emissivity chosen for the receiver surface is based on that temperature. Specifically, the receiver surface properties are those measured for a black nickel coating. The reflectivity is that quoted by the manufacturer for Alzac* aluminum, which is available in sheet form and which has been proposed as a suitable reflector material. The optical properties of the envelope are characteristic of Corning Glass Works Code 7052 glass. The emissivities of the envelope silvering and the outer surface of the insulation are easily obtained with current techniques.

The convection heat transfer coefficient for the outermost surface is determined for air flowing at 5 miles per hour normal to a heated tube. To maximize the heat transfer to the working fluid, turbulent flow is maintained in the receiver. The film coefficient inside the receiver is characteristic of Therminol-66† flowing at 2.5 feet per second.

A maximum solar insolation characteristic of Albuquerque, New Mexico, is 318 Btu/ft^2-hr. This is the flux taken normal to the incoming radiation. The present study considers the performance of the solar collectors operating at a steady state with this maximum input; and efficiencies, or other performance data, must be adjusted before they can be used to predict system performance under other conditions.

The radiation heat transfer from the receiver to the envelope is analyzed as a radiosity network of the eight receiver surface nodes and eight envelope surface nodes. Such a solution requires the emissivity and area of each of the participating surfaces and the matrix of shape factors, i.e., the fractions of energy emitted by each of the surfaces which are intercepted by each of the surfaces. In general, the shape factor matrix for the present problem is a 16x16 matrix. However, with the areas of the surfaces and the reciprocity relation between areas and shape factors, half the matrix can be uniquely determined from the other half, so that only half the shape factor matrix plus the principal diagonal is required to specify the problem. The receiver surface is convex so that none of the nodes can radiate to itself or to another receiver node. If it is assumed that, because the envelope surface nodes are

*Registered trademark of Aluminum Company of America.

†Registered trademark of Monsanto Chemical Corporation.

nearly uniform in temperature, there is negligible heat transfer by radiation among them and if the fact that each envelope surface node can see itself is ignored, the corresponding shape factors may be taken as zero. Therefore, only an 8x8 section of the 16x16 matrix need be specified, all other elements being either zero or calculable. The required shape factors then are those related to the radiation of the receiver nodes to the envelope nodes.

To develop these shape factors it is assumed that each surface node on the receiver radiates only to five nodes centered directly opposite on the envelope. For example, Node 4 in Figure 2 radiates only to Nodes 18-22. Since all energy radiated by the receiver node must be intercepted by the five envelope nodes, the sum of the five shape factors must be one. For those nodes near the plane of symmetry, that boundary of the problem appears as a perfect mirror, and the shape factors must account for the fact that, as an example, Node 9 radiates to Node 18 directly and by reflection from the adiabatic boundary. The shape factors relative to the nodes as shown in Figure 2 are given in Table 2.

Table 2. Radiative Shape Factors

Node	17	18	19	20	21	22	23	24
9	.55	.34	.11	0	0	0	0	0
10	.34	.32	.23	.11	0	0	0	0
11	.11	.23	.32	.23	.11	0	0	0
12	0	.11	.23	.32	.23	.11	0	0
13	0	0	.11	.23	.32	.23	.11	0
14	0	0	0	.11	.23	.32	.23	.11
15	0	0	0	0	.11	.23	.32	.34
16	0	0	0	0	0	.11	.34	.55

The required receiver diameter for each focal length is determined by the maximum distance from the reflector surface to the focal line, i.e., the distance from the edge of the reflector to the centerline of the receiver. Since the sun subtends an angle of 32 minutes and if it is assumed that the mirror slope error is ±15' and the tracking error is ±15', the receiver must be sized to subtend at least 92' in order to intercept the somewhat divergent reflected solar flux. A study by Edwards, et al. [11], concludes that the incident angle of solar radiation should be less than 60° from the normal to the receiver surface for effective absorption. Therefore the receiver tube diameter is given by

$$D = \frac{2r \sin(92'/2)}{\sin 60^\circ} \qquad (1)$$

where r is the distance from the reflector lip to the receiver centerline. For parabolic cylinders the distance from the focal line to the edge is given by

$$r = \frac{W}{2 \sin A_r} \tag{2}$$

where W is the width of the collector and A_r is the receiver rim angle.

With Equations 1 and 2 the outside diameters of four receivers, with rim angles of 115°, 90°, 70°, and 45°, have been determined. For each of these it has been assumed that (1) the receiver wall thickness is 0.0625 in., (2) there is a 0.25 in. gap between the receiver and envelope, (3) the glass envelope is 0.125 in. thick, and (4) the outside insulation, where it is included, is 0.5 in. thick. The data required to input these designs to the computer program are given in Table 3.

Table 3. Design Data for Receivers

Rim Angle	115°	90°	70°	45°
Receiver Diameter	1.841	1.669	1.776	2.359
R_1	.858	.772	.825	1.117
R_2	.921	.835	.888	1.180
R_3	1.171	1.084	1.138	1.430
R_4	1.296	1.209	1.263	1.555
R_5	1.796	1.709	1.763	2.055
Window Angle	158°	132°	112°	91°
Segments of silvering and insulation	1	2	3	4

Because of the divergence of the reflected light rays, the receiver is illuminated over an angle greater than the rim angle. As described above, each receiver is sized such that it may be illuminated as much as 60° more than the rim angle. However, even for rim angles as large as 115°, not all of the envelope receives reflected insolation. This analysis considers the performance of receiver designs which employ silvering on the inside surface and insulation on the outside surface of the envelope to minimize thermal losses through the unilluminated part of the envelope.

The size of the window through the envelope may be determined using Figure 3. The angle AFE is the rim angle, and the point B is the uppermost point

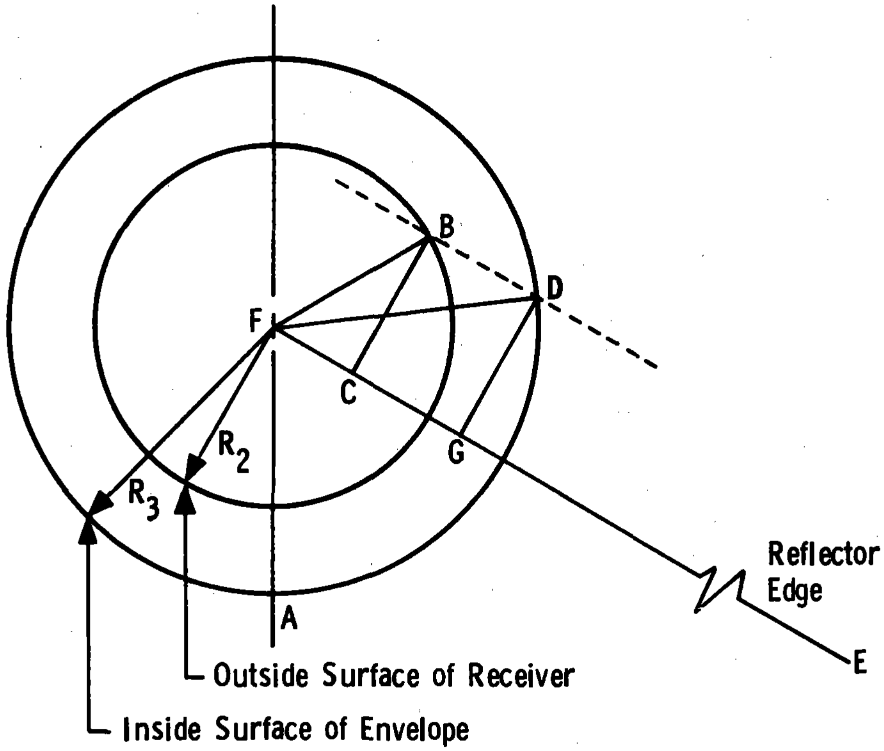

Figure 3. Determination of window angle

which receives illumination. Constructing through B a line parallel to FE gives the point D which is approximately the boundary of the illuminated part of the envelope. (To be exact, the lines FE and BD meet at the reflector edge and diverge with an angle of 46' between them.) The angle AFD subtended by the window, A_w, is then given by

$$A_w = A_r + \sin^{-1}\left[\frac{R_2 \sin 60°}{R_3}\right] \qquad (3)$$

Because the thermal model is a nodal network to be solved numerically, the thermal protection may be considered only as covering an integer number of segments. The window angles determined from Equation 3 for receivers with rim angles of 115°, 90°, 70°, and 45° allow silvering and insulation very nearly over 1, 2, 3, and 4 segments, respectively.

The heat input to the receiver must be determined for each segment in each design. A study is underway at Sandia Laboratories to develop a ray-tracing, Monte Carlo technique to calculate these heat flux distributions. For the present analysis it is assumed that each segment within the rim angle is fully exposed and it is given a scale factor of 1.0, while the next three segments are partially illuminated and are given scale factors of 0.8, 0.4, and 0.1 sequentially. The heat input is then distributed among the eight segments according to the scale factors.

The thermal model represents one half of the receiver and the incident radiation is attenuated by the reflectivity of the reflector, the transmissivity of the envelope, and the absorptivity of the receiver surface. Therefore, the solar input to the receiver in a collector 9.0 ft wide is 1.257 Btu/min per inch of length for the baseline conditions presented in Table 1. This heat input also must be reduced to account for the receiver's shading the reflector. The resulting heat input distributions are shown in Table 4 for the four cases.

Table 4. Heat Input Distributions

Node No.	115°	90°	70°	45°
1	.0199	0	0	0
2	.0773	.0235	0	0
3	.155	.0927	.0290	0
4	.194	.185	.113	.0370
5	.194	.231	.226	.145
6	.194	.231	.283	.292
7	.194	.231	.283	.366
8	.194	.231	.283	.366

III. Results and Conclusions

Optimum Rim Angle for Baseline Input

The computer model has been run for each of the four receiver designs for the baseline conditions, and the results are shown in Table 5. The heat transfer rates are given per inch of length in the axial direction. The heat ratio is the ratio of the heat transferred to the working fluid to the heat absorbed at the receiver surface. The collector efficiency is the ratio of the heat transferred to the working fluid to the insolation intercepted by the collector. The data show that for a given collector width intermediate rim angles give better performance for the baseline conditions than either large or small rim angles. Further discussion is deferred until some data other than the baseline have been considered. The present analysis has been compared to a previous treatment [8] by considering a common problem. The problem chosen for the comparison is the 115° rim angle case presented above, with two exceptions. Because Edenburn's analysis is one-dimensional and cannot consider an outer layer of insulation, the insulation is deleted completely, and the radii of the various components of the receiver were

Table 5. Results for Baseline Conditions

	115°	90°	70°	45°
Heat to Receiver (Btu/min)	1.224	1.225	1.216	1.206
Heat to Fluid (Btu/min)	.900	.943	.938	.882
Convection Loss (Btu/min)	.236	.205	.206	.245
Radiation Loss (Btu/min)	.089	.077	.072	.078
Heat Ratio (%)	73.52	76.98	77.14	73.18
Collector Efficiency (%)	45.27	47.45	47.20	43.40

modified slightly to utilize a standard pipe size for the receiver tube. The results of the comparison are shown in Figure 4 as a function of the emissivity of the receiver surface; the two models shown excellent agreement. A listing of the program for the 90° rim angle case at baseline conditions is shown in the Appendix.

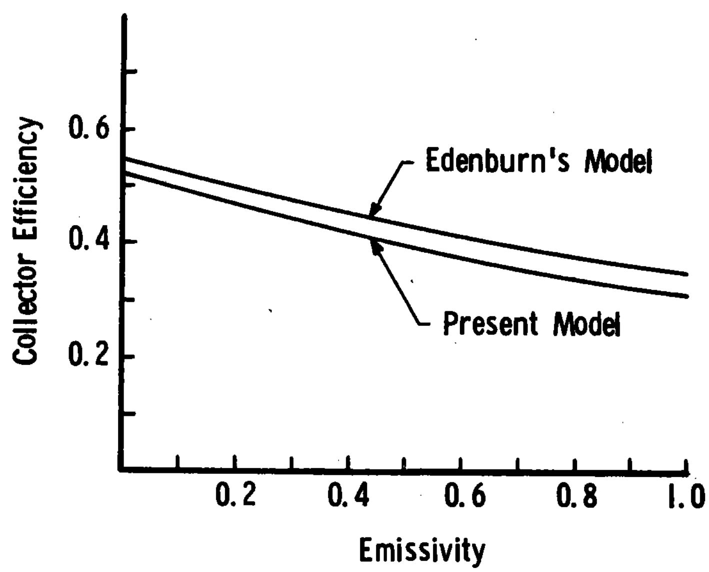

Figure 4. Collector performance as a function of the emissivity of the receiver surface

One of the most active areas of solar energy research is the effort to reduce the emittance of the receiver surface while maintaining a high solar absorptance. The performance of each of the receiver designs was examined over the full range of possible emissivity values, holding all other parameters at the baseline values. Table 6 shows the resulting collector efficiencies, and the preference for intermediate focal lengths indicated above is

Table 6. Collector Efficiencies for Varying Emissivity

Emissivity	115°	90°	70°	45°
0.0	52.95	53.92	53.36	51.26
0.1	50.12	51.47	50.94	48.46
0.2	47.57	49.33	48.94	46.24
0.3	45.27	47.45	47.20	44.40
0.4	43.19	45.77	45.68	42.82
0.5	41.31	44.28	44.33	41.43
0.6	39.60	42.91	43.12	40.20
0.7	38.04	41.67	42.02	39.10
0.8	36.60	40.55	41.03	38.11
0.9	35.30	39.52	40.11	37.18
1.0	34.09	38.56	39.27	36.39

substantiated at all emissivities. Furthermore, the data indicate that the performance of the collectors is not a strong function of the rim angle in the intermediate zone, i.e., small deviations from 90° do not precipitate large increases in thermal losses. Changes in the thermal performance are quite small so that other considerations, such as fabricability, may dictate rim angles smaller or larger than 90° provided that the departure from 90° is not extreme. Since recent laboratory measurements have shown that emissivities on the receiver surface of 0.3 or less can be expected, the 90° rim angle receiver design is selected as the preferred configuration.

Variation from Baseline Input

In addition to meeting the primary objective of this study, i.e., to determine the effect of rim angle on receiver performance, the computer model which had been developed has been used to examine further the sensitivity of the collector performance to variations in some of the design parameters. Some notable results have been obtained.

Much has been made of the importance of improving the ratio of absorptivity in the visible to emissivity in the infrared for receiver surfaces. If collector performance is equated with this ratio, lowering the emissivity becomes increasingly important as the emissivity approaches zero, giving very large values of the ratio. However, Figure 5 shows the effects of improving both the absorptivity and the emissivity independently rather than considered together as a ratio. These data, for the 90° rim angle receiver design and the baseline conditions except for absorptivity and emissivity, reveal that the improvement in collector performance for a unit decrease in emissivity

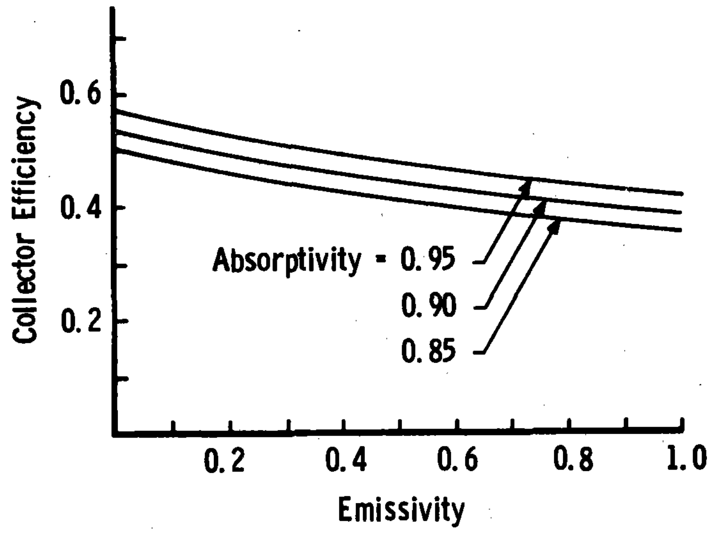

Figure 5. Effects of receiver absorptivity and emissivity on collector efficiency

is not a strong function of emissivity, i.e., changing the emissivity from 0.6 to 0.5 has approximately the same quantitative effect as changing from 0.2 to 0.1. Furthermore, collector improvements by incrementally increasing absorptivity are more effective and probably much less difficult than corresponding decreases in emissivity, e.g., a 0.05 increase in absorptivity achieves the same result as decreasing the emissivity by 0.20. These facts may be obscured by considering the data of Figure 5 in terms of the ratio of absorptivity to emissivity only. In other words, any reference to the absorptivity-to-emissivity ratio for a given surface should be related to the value of one or the other of the properties.

To this point only the performance with maximum solar input has been discussed. The designs have been reexamined at lower insolation rates, and no qualitative difference from the data presented in Table 6 has been found. The quantitative effect for the 90° rim angle receiver at the baseline conditions is shown in Table 7.

Table 7. Collector Performance for Partial Solar Input

Insolation Rate (Btu/hr-ft^2)	318	223	156	109
Efficiency (%)	47.45	41.85	33.93	22.61

The 90° rim angle design with the baseline conditions was used to evaluate the effects of other parametric variations. Reducing the working fluid temperature improved the efficiency of the collector. Fluid temperatures of 600°F, 525°F, and 450°F yielded collector efficiencies of 47.45, 50.41, and 52.98, respectively. In the range of primary interest, reducing the emissivity of the envelope silvering from 0.2 to 0.01 had a negligible impact. However, this reflective coating becomes more important as the emissivity of the receiver increases and for designs with smaller rim angles. The radiation sink temperature was changed from 77°F to -100°F and the insulation thickness was doubled. Neither of these variations had a significant effect upon the receiver performance.

IV. Discussion

The primary conclusion to be drawn from this study is that, for the conditions described herein, the optimum rim angle is approximately 90°. The conclusion is stated in approximate terms because numerical techniques have been used which preclude the consideration of a continuum of rim angles. This is sufficient for present purposes, however, because the data indicate that receiver performance is not a strong function of rim angle in the vicinity of 90°. In the construction of solar collector systems, other considerations, such as fabricability, may override absolute thermal optimization. The fact that the optimum design is somewhat dependent upon the properties of the various collector materials and surfaces also causes some uncertainty in the choice of an absolute optimum. For example, Table 6 shows that the optimum rim angle decreases as the receiver emissivity increases. At the present time, neither the materials nor their properties can be specified with precision.

The thermal losses from receivers are functions of the receiver surface area so that, for symmetric receivers, better performance is given by designs which permit smaller receivers. By considering asymmetric designs, this study has shown that the addition of thermal protective measures to the unilluminated portion of the envelope has the effect of offsetting, but not completely, the adverse effect of the larger receiver diameters required for smaller rim angles. Therefore a broader range of rim angles is available, within which collector performance is very near the maximum, than would be possible without the insulation and reflective coating.

Because the size of the receiver is so important it may be worthwhile in future studies to investigate further optimization within the constraint of a 90° rim angle. For instance, the receiver sizes in this study were selected such that the reflected flux had a maximum angle of incidence of 60° on the receiver. Perhaps this criterion could be relaxed in favor of a smaller receiver.

The computer program developed in this study has met the objective of determining the optimum rim angle for the conditions of interest. It will continue to be a useful tool as receiver designs are evaluated relative to other criteria and as experimental data from specific receivers are analyzed.

REFERENCES

1. R. B. Pope, et al., "A Combination of Solar Energy and the Total Energy Concept--The Solar Community," Proceedings of the Eighth Intersociety Energy Conversion Engineering Conference, Philadelphia, Pennsylvania, August 13-17, 1973, pp. 304-311.

2. R. B. Pope and W. P. Schimmel, Jr., "The Solar Community and the Cascaded Energy Concept Applied to a Single House and a Small Subdivision--A Status Report," SLA-73-0357, Sandia Laboratories, Albuquerque, New Mexico, May 1973.

3. W. H. McCulloch, et al., "The Solar Community--Energy for Residential Heating, Cooling, and Electric Power," American Association for the Advancement of Science Annual Meeting, San Francisco, California, February 25 - March 1, 1974.

4. Kamal-Eldin Hassan and Mohamed Fawzi El-Refaie, "Theoretical Performance of Cylindrical Parabolic Solar Concentrators," Solar Energy, Vol. 15, No. 3, September 1973, pp. 219-244.

5. G. O. G. Löf, et al., "Energy Balances on a Parabolic Cylinder Solar Collector," Transactions of the ASME: Journal of Engineering for Power, January 1962, pp. 24-32.

6. R. B. Pope and W. P. Schimmel, Jr., "An Analysis of Linear Focused Collectors for Solar Power," Proceedings of Eighth Intersociety Energy Conversion Engineering Conference, Philadelphia, Pennsylvania, August 13-16, 1973, pp. 353-359.

7. "Research Applied to Solar-Thermal Power Systems," Semi-Annual Progress Report, NSF Grant GI-34871, Report NSF/RANN/SE/GI-34871/PR/73/2, University of Minnesota and Honeywell, July 31, 1973, pp. 62-73.

8. M. W. Edenburn, "Performance of a Focusing Cylindrical Parabolic Solar Energy Collector: Analysis and Computer Program," SLA-74-0031, Sandia Laboratories, Albuquerque, New Mexico, April 1974.

9. D. R. Lewis, et al., "Chrysler Improved Numerical Differencing Analyzer for 3rd Generation Computers," Technical Note TN-AP-67-287, Chrysler Corporation Space Division, New Orleans, Louisiana, October 20, 1967.

10. Frank Kreith, Principles of Heat Transfer, 2nd Edition, International Textbook Company, Scranton, Pennsylvania, 1965.

11. D. K. Edwards, et al., "Spectral and Directional Thermal Radiation Characteristics of Selective Surfaces for Solar Collectors," Solar Energy, Vol. 6, No. 1, January-March 1962.

APPENDIX

The following is a listing of the program deck for the 90° rim angle case at the baseline conditions as submitted for the CDC-6600 computer. The deck consists of control cards, Fortran subroutines to generate the input data for the CINDA analysis and to give the results in a format designed specifically for this study, and the data input cards for CINDA-3G, the generalized heat transfer code in use at Sandia Laboratories.

```
REC,CM77000,T300.                               WH MCCULLOCH   BLDG 836   BOX 204
ACCOUNT,S464684435,D1543,G3500,A0005501,RT,KUNC.
ATTACH,PRELIB,CINDA,CY=30.
FTN.
REWIND,OUTPUT.
COLLECT,PROGRAM=PREPRO,CINPRO,PRELIB,FTNLIB.
MAP,OFF.
CINPRO.
UNLOAD,CINPRO.
REWIND,TAPE13.
FTN,I=TAPE13,R=0,L=NOLIST.
UNLOAD,TAPE13.
ATTACH,RANLIB,CINDA,CY=50.
COLLECT,LGO,RANLIB,FTNLIB.
LGO.
COMMENT.  ***  CINDA JOB COMPLETED  ***
EXIT.
COMMENT.  ***  ABNORMAL TERMINATION  ***
'
      SUBROUTINE SETUPP(R,CONMPY,AREC,AENV)
      DIMENSION R(5),CONMPY(17)
      CONMPY(1)=.393*R(1)
      CONMPY(2)=.785*(R(1)+.25*(R(2)-R(1)))/(R(2)-R(1))
      CONMPY(3)=.785*(R(2)-.25*(R(2)-R(1)))/(R(2)-R(1))
      CONMPY(4)=.785*(R(2)+.25*(R(3)-R(2)))/(R(3)-R(2))
      CONMPY(5)=.785*(R(3)-.25*(R(3)-R(2)))/(R(3)-R(2))
      CONMPY(6)=.785*(R(3)+.25*(R(4)-R(3)))/(R(4)-R(3))
      CONMPY(7)=.785*(R(4)-.25*(R(4)-R(3)))/(R(4)-R(3))
      CONMPY(8)=.785*(R(4)+.25*(R(5)-R(4)))/(R(5)-R(4))
      CONMPY(9)=.785*(R(5)-.25*(R(5)-R(4)))/(R(5)-R(4))
      CONMPY(10)=5.093*(R(2)-R(1))/(R(2)+R(1))
      CONMPY(11)=5.093*(R(3)-R(2))/(R(3)+R(2))
      CONMPY(12)=5.093*(R(4)-R(3))/(R(4)+R(3))
      CONMPY(13)=5.093*(R(5)-R(4))/(R(4)+R(3))
      CONMPY(14)=.393*R(4)
      CONMPY(15)=.393*R(5)
      CONMPY(16)=.78E-13*R(4)
      CONMPY(17)=.78E-13*R(5)
      AREC=.393*R(2)
      AENV=.393*R(3)
      RETURN
      END
```

```
      SUBROUTINE PRNTOT(T,XK1,TTEST,VTEST,XK9)
      DIMENSION T(1)
      CALL TOPLIN
      PRINT 20
   20 FORMAT(5X,*SEGMENT NUMBER*,9X,*1*,11X,*2*,11X,*3*,11X,*4*,11X,
     1*5*,11X,*6*,11X,*7*,11X,*8*,/)
      PRINT 21,(T(I),I=65,72)
   21 FORMAT(5X,*OUTER SURFACE *,8(4X,F8.2)/)
      PRINT 22,(T(I),I=25,32)
   22 FORMAT(5X,*INSULATION    *,8(4X,F8.2)/)
      PRINT 23,(T(I),I=57,64)
   23 FORMAT(5X,*  INTERFACE   *,8(4X,F8.2)/)
      PRINT 24,(T(I),I=17,24)
   24 FORMAT(5X,*ENVELOPE      *,8(4X,F8.2)/)
      PRINT 23,(T(I),I=49,56)
      PRINT 25,(T(I),I=9,16)
   25 FORMAT (5X,*ANNULUS       *,8(4X,F8.2)/)
      PRINT 23,(T(I),I=41,48)
      PRINT 26,(T(I),I=1,8)
   26 FORMAT(5X,*RECEIVER      *,8(4X,F8.2)/)
      PRINT 27,(T(I),I=33,40)
   27 FORMAT(5X,*INNER SURFACE *,8(4X,F8.2)//)
      X1=100.*XK9/XK1
      X2=100.*TTEST/XK1
      X3=100.*VTEST/XK1
      PRINT 28,XK1
   28 FORMAT(5X,*HEAT INPUT TO RECEIVER SURFACE = *,F8.4,* BTU/MIN*,//)
      PRINT 29,T(73),T(74),T(75)
   29 FORMAT(5X,*FLUID TEMPERATURE       = *,F8.2,5X,*AMBIENT TEMP     = *,
     1F8.2,5X,*RADIATION SINK TEMP = *,F8.2,5X,*FAHRENHEIT*,/)
      PRINT 30,XK9,TTEST,VTEST,X1,X2,X3
   30 FORMAT(5X,*HEAT TRANSFER TO FLUID = *,F8.4,5X,*CONVECTION LOSS = *,
     1F8.4,5X,*RADIATION LOSS        = *,F8.4,5X,*BTU/MIN*,/,30X,*(*,
     2F7.2,*)*,22X,*(*,F7.2,*)*,26X,*(*,F7.2,*)*,4X,*PERCENT*)
      RETURN
      END
      SUBROUTINE TOPLIN
      COMMON /FIXCON/ N(51)
      COMMON /TITLE/ H(60)
       DATA          K/0/
      N(28) = 7
      N(29) = N(29) + 1
      IF(K.NE.0)  GO TO 50
      K = 1
      CALL HOROLOG(IT,IIT,DTE)
   50 CONTINUE
      WRITE(6,100) DTE,N(29),H
  100 FORMAT(1H0,/,6H DATE ,A10,5X,
     1         52HCINDA-3G (SANDIA LABORATORIES CDC 6600 VERSION)  -  ,
     2         40HNUMERICAL DIFFERENCING ANALYZER -  FD228,5X,
     3          4HPAGE,I7,//5X,20A6/5X,20A6/5X,20A6/)
      RETURN
      END
NOT RECALL
        BCD 3THERMAL LPCS
        BCD 9ASYMMETRIC RECEIVER ANALYSIS-INTERMEDIATE FOCAL LENGTH
        END
        BCD 3NODE DATA
```

```
REM RECEIVER NODES
GEN 1,8,1,0.0,1.,1.,1.,1.
REM AIR GAP NODES
GEN 9,8,1,0.0,1.,1.,1.,1.
REM ENVELOPE NODES
GEN 17,8,1,0.0,1.,1.,1.,1.
REM INSULATION NODES
GEN 25,8,1,0.0,1.,1.,1.,1.
REM INTERFACIAL NODES
GEN 33,40,1,0.0,1.,1.,1.,-1.
REM FLUID AND AMBIENT AIR
    -73,0.0,0.0,-74,0.0,0.0
REM RADIATION SINK NODE
    -75,0.0,0.0
END
BCD 3CONDUCTOR DATA
REM RADIAL CONDUCTORS
GEN 1,8,1,33,1,1,1,1.,1.,1.,1.
GEN 9,8,1,1,1,41,1,1.,1.,1.,1.
GEN 17,8,1,41,1,9,1,1.,1.,1.,1.
GEN 25,8,1,9,1,49,1,1.,1.,1.,1.
GEN 33,8,1,49,1,17,1,1.,1.,1.,1.
GEN 41,8,1,17,1,57,1,1.,1.,1.,1.
GEN 49,8,1,57,1,25,1,1.,1.,1.,1.
GEN 57,8,1,25,1,65,1,1.,1.,1.,1.
REM CIRCUMFERENTIAL CONDUCTORS
GEN 65,7,1,1,1,2,1,1.,1.,1.,1.
GEN 73,7,1,9,1,10,1,1.,1.,1.,1.
GEN 80,7,1,17,1,18,1,1.,1.,1.,1.
GEN 87,7,1,25,1,26,1,0.,1.,1.,1.
REM RADIAL CONDUCTORS TO FLUIDS
GEN 94,8,1,33,1,73,0,1.,1.,1.,1.
GEN 102,8,1,65,1,74,0,1.,1.,1.,1.
REM RADIATION CONDUCTORS
GEN -235,8,1,65,1,75,0,1.,1.,1.,1.
END
BCD 3CONSTANTS DATA
    NLOOP,9000,BALENG,.06,LAXFAC,50
    1,0.,2,0.,3,0.,4,0.,5,0.,6,0.,7,0.,8,0.,9,0.
END
BCD 3ARRAY DATA
    1  $CONCENTRIC RADII OF MATERIALS(IN)
    .7718,.8343,1.0843,1.2093,1.7093,END  $90 CASE
    2  $CONVECTION COEFFICIENTS, FLUID AND AMBIENT(BTU/IN**2-MIN-F)
    1.9E-2,3.98E-4,END
    3  $NO. SEGMENTS FOR SILVERING AND INSULATION
      2,2,1,END
    4  $CONDUCTIVITY OF RECEIVER(BTU/MIN-IN-F)
    32.,.0368,212.,.0361,572.,.0347,932.,.0306,END
    5  $CONDUCTIVITY OF AIR
    0.,1.85E-5,100.,2.14E-5,300.,2.68E-5,600.,3.47E-5,END
    6  $CONDUCTIVITY OF ENVELOPE
    0.,6.25E-4,600.,6.25E-4,END
    7  $CONDUCTIVITY OF INSULATION
    0.,7.08E-5,600.,7.08E-5,END
    8  $RHO-CP FOR RECEIVER(BTU/IN**3-F)
    0.,.0312,600.,.0312,END
    9  $RHO-CP FOR AIR
    0.,9.86E-6,600.,9.86E-6,END
```

```
        10  $RHO-CP FOR ENVELOPE
        0.,.0197,600.,.0197,END
        11  $RHO-CP FOR INSULATION
        0.,.00316,600.,.00316,END
        12  $EMISSIVITY OF RECEIVER VS TEMPERATURE(F)
        0.,.3,600.,.3,END
        13  $EMISSIVITY OF SILVERING
        0.,.2,600.,.2,END
        14  $EMISSIVITY OF ENVELOPE VS TEMPERATURE (F)
        0.,.9,600.,.9,END
        15  $INPUT TO SEGMENTS OF RECEIVER(BTU/MIN)(FROM TOP DOWN)
        0.,.02346,.09266,.185,.231,.231,.231,.231,END
        16  $CONDUCTION MULTIPLIERS FROM SETUP
        SPACE,17,END
        17  $INITIAL TEMPERATURE FOR COLLECTOR AND FLUID, AMBIENT,
   REM          RADIATION SINK TEMPERATURES(F)
        70.0,600.,77.,77.,END
        18  $EMISSIVITY OF INSULATION SURFACE VS TEMPERATURE(F)
        0.,.2,600.,.2,END
        30  $TEMPERATURE-Q ARRAY (RADIOSITY NETWORK)
        SPACE,16,END
        31  $AREA ARRAY (RADIOSITY NETWORK)
        SPACE,16,END
        32  $EMISSIVITY ARRAY (RADIOSITY NETWORK)
        SPACE,16,END
        33  $AREA*SHAPE FACTORS FOR ENCLOSURE
        SPACE,138,END
   END
   BCD 3EXECUTION
F     DIMENSION X(300)
F     NDIM = 300
F     NTH = 0
        SETUPP(A1+1,A16+1,RTEST,STEST)
   REM INPUT TEMPERATURES
        STFSQS(A17+1,72,T1)
        SCALE(1.,A17+2,T73,A17+3,T74,A17+4,T75)
F     LTEST=0
        CINDSR
   END
   BCD 3VARIABLES 1
   REM SET CONDUCTANCE VALUES FOR CONNECTORS
        GENCGC(8,1,T33,1,T1,1,A4,A16+2,G1)
        GENCGC(8,1,T1,1,T41,1,A4,A16+3,G9)
        GENCGC(8,1,T41,1,T9,1,A5,A16+4,G17)
        GENCGC(8,1,T9,1,T49,1,A5,A16+5,G25)
        GENCGC(8,1,T49,1,T17,1,A6,A16+6,G33)
        GENCGC(8,1,T17,1,T57,1,A6,A16+7,G41)
        STFSEP(A3+2,ITEST)
F     IF(ITEST .LE. 0) GO TO 21
        GENCGC(A3+2,1,T57,1,T25,1,A7,A16+8,G49)
        GENCGC(A3+2,1,T25,1,T65,1,A7,A16+9,G57)
F  21 CONTINUE
        GENCGC(7,1,T1,1,T2,1,A4,A16+10,G65)
        GENCGC(7,1,T9,1,T10,1,A5,A16+11,G73)
        GENCGC(7,1,T17,1,T18,1,A6,A16+12,G80)
        STFSEP(A3+3,JTEST)
F     IF(JTEST .LE. 0) GO TO 22
        GENCGC(A3+3,1,T25,1,T26,1,A7,A16+13,G87)
F  22 CONTINUE
```

```
        REM SET CONDUCTANCE VALUES FOR CONVECTION CONNECTORS
            MLTPLY(A16+1,A2+1,G94)
            STFSEQ(G94,8)
            MLTPLY(A16+14,A2+2,G102)
            STFSEQ(G102,8)
            MLTPLY(A16+15,A2+2,G102)
            STFSEQ(G102,A3+2)
        REM VALUES FOR RADIATION-TO-SINK CONNECTORS
            D1D1IM(8,T65,A14,A16+16,G235)
            D1D1IM(A3+2,T65,A18,A16+17,G235)
        REM BUILD ARRAYS FOR RADIOSITY NETWORK SOLUTION
            STFSQS(0.,138,A33+1)
            STFSQS(RTEST,8,A31+1)
            STFSQS(STEST,8,A31+9)
            STFSEP(16,A33+1)
            STFSEP(.198E-12,A33+2)
            SCALE(RTEST,.55,A33+11,.34,A33+12,.11,A33+13)
            SCALE(RTEST,.34,A33+26,.32,A33+27,.23,A33+28,.11,A33+29)
            SCALE(RTEST,.11,A33+40,.23,A33+41,.32,A33+42,.23,A33+43
            .11,A33+44)
            SCALE(RTEST,.11,A33+54,.23,A33+55,.32,A33+56,.23,A33+57
            .11,A33+58)
            SCALE(RTEST,.11,A33+67,.23,A33+68,.32,A33+69,.23,A33+70
            .11,A33+71)
            SCALE(RTEST,.11,A33+79,.23,A33+80,.32,A33+81,.23,A33+82
            .11,A33+83)
            SCALE(RTEST,.11,A33+90,.23,A33+91,.32,A33+92,.34,A33+93)
            SCALE(RTEST,.11,A33+100,.34,A33+101,.55,A33+102)
            D1DG1I(8,T41,A12,A32+1)
            D1DG1I(8,T49,A14,A32+9)
            STFSEP(A3+1,KTEST)
F      IF (KTEST .LE. 0)  GO TO 23
            D1DG1I(A3+1,T49,A13,A32+9)
F   23 CONTINUE
            SHFTV(16,T41,A30+1)
        REM RADIOSITY NETWORK SOLUTION
            IRRADE(A31,A32,A33,A30)
            SHFTV(16,A30+1,Q41)
        REM ADD HEAT INPUT TO RECEIVER SURFACE
            ADDARY(8,A15+1,Q41,Q41)
        END
        BCD 3VARIABLES 2
        END
        BCD 3OUTPUT CALLS
F      IF (LTEST .LE. 0)  GO TO 41
            QMETER(T65,T74,G102,K1)
            QMETER(T66,T74,G103,K2)
            QMETER(T67,T74,G104,K3)
            QMETER(T68,T74,G105,K4)
            QMETER(T69,T74,G106,K5)
            QMETER(T70,T74,G107,K6)
            QMETER(T71,T74,G108,K7)
            QMETER(T72,T74,G109,K8)
            SUMARY(8,K1,TTEST)
            RDTNQS(T75,T65,G235,K1)
            RDTNQS(T75,T66,G236,K2)
            RDTNQS(T75,T67,G237,K3)
            RDTNQS(T75,T68,G238,K4)
            RDTNQS(T75,T69,G239,K5)
```

```
               RDTNQS(T75,T70,G240,K6)
               RDTNQS(T75,T71,G241,K7)
               RDTNQS(T75,T72,G242,K8)
               SUMARY(8,K1,VTEST)
               QMETER(T33,T73,G94,K1)
               QMETER(T34,T73,G95,K2)
               QMETER(T35,T73,G96,K3)
               QMETER(T36,T73,G97,K4)
               QMETER(T37,T73,G98,K5)
               QMETER(T38,T73,G99,K6)
               QMETER(T39,T73,G100,K7)
               QMETER(T40,T73,G101,K8)
               SUMARY(8,K1,K9)
               SUMARY(8,A15+1,K1)
               PRNTOT(T1,K1,TTEST,VTEST,K9)
F         LTEST=0
F         GO TO 42
F      41 LTEST=1
F      42 CONTINUE
           END
           BCD 3END OF DATA
```

DISTRIBUTION:

Robert San Martin
Department of Mechanical Engineering
New Mexico State University
Las Cruces, New Mexico 88003

M. W. Wildin
Department of Mechanical Engineering
University of New Mexico
Albuquerque, New Mexico 87106

1540 T. B. Lane
1543 H. C. Hardee
1543 D. O. Lee
1543 W. H. McCulloch (50)
2324 J. P. Abbin, Jr.
2441 G. W. Gobeli
3620 R. S. Wilson
3622 L. G. Rainhart
4010 M. J. Sektnan
4700 D. B. Shuster
4734 V. L. Dugan
5111 S. T. Picraux
5700 J. H. Scott
5710 G. E. Brandvold
5712 R. H. Braasch (4)
5712 S. Thunborg
5712 G. W. Treadwell (10)
5717 R. P. Stromberg (4)
5824 R. W. Lynch
5832 R. W. Rohde
5834 D. M. Mattox
5842 R. C. Heckman
8110 A. N. Blackwell
8184 A. C. Skinrood
8184 C. T. Yokomizo
9331 N. R. Keltner
9474 L. W. Scully
8266 E. A. Aas (2)
3141 A. M. Torneby (5)
3151 W. F. Carstens (3)
For AEC/TIC (Unlimited Release)

Org.	Bldg.	Name	Rec'd by*	Org.	Bldg.	Name	Rec'd by*

*Recipient must initial on classified documents.